INSTITUTE FOR FUSION STUDIES

DOE/ET-53088-518 IFSR #518

Continuum Damping of High Mode Number Toroidal Alfvén Waves

M.N. ROSENBLUTH
Department of Physics
University of California
San Diego, CA 92093

H.L. BERK, D.M. LINDBERG, AND J.W. VAN DAM
Institute for Fusion Studies
The University of Texas at Austin
Austin, Texas 78712

August 1991

THE UNIVERSITY OF TEXAS

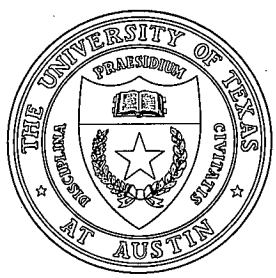

AUSTIN

Continuum Damping of High Mode Number Toroidal Alfvén Waves

M.N. Rosenbluth,[1] H.L. Berk,[2] D.M. Lindberg,[2] and J.W. Van Dam[2]

[1]Department of Physics, University of California, San Diego, CA 92093
and General Atomics, San Diego, CA 92138
[2]Institute for Fusion Studies, The University of Texas at Austin,
Austin, TX 78712

Abstract

An asymptotic theory is developed to determine the continuum damping of short-wavelength Toroidal Alfvén Eigenmodes, which is essential for ascertaining thresholds for alpha particle driven instability in ignited tokamaks.

Magnetic fusion research has finally reached the point at which large scale thermonuclear burning experiments can be undertaken. The introduction of D-T fuel into TFTR and JET is being planned and several larger experiments such as BPX, ITER, NET and FER have been proposed to attain full self-sustaining burn. Thus it is essential to think about novel physics features that may arise from the presence of large numbers of fusion product alpha particles whose speeds are greater than the Alfvén speed $v_A = B_0/(4\pi\rho)^{1/2}$. Some effects have already been seen from superthermal fast ions produced by neutral beams or rf heating.[1,2] It has been pointed out[3,4] that toroidal coupling of the alphas to the Alfvén wave might lead to instability and possible diffusive loss of the alpha particles. A principal uncertainty in estimating the critical threshold for the instability lies in calculating the damping rate of the Alfvén waves. In a sheared magnetic field these waves are highly localized at the surface $\omega = k_{\|} v_A$ and strongly damped in most cases. An exception occurs for the so-called Toroidal Alfvén Eigenmodes (TAE)[5] where, due to the periodic nature of the toroidal

field, gaps can arise in the continuum frequency spectrum of localized modes, within which discrete modes (undamped in lowest order) exist and can be alpha particle destabilized. Since the destabilization is weak, it is also necessary to calculate the damping with some precision. Within the ideal MHD equations one can describe damping independent of the detailed dissipation mechanism from the structure of the Alfvén continuum resonance.[6-8] The purpose of this letter is to present a detailed asymptotic linear theory for the damping of short wavelength TAE modes in a large aspect ratio tokamak.

We limit ourselves here to nearly circular equilibria and assume small inverse aspect ratio r/R, low β, and high average poloidal mode number m_0 (so $d/dr \gg 1/r$ while $m_0\varepsilon$ is finite).

The frequency of a linearized wave is determined from the stationarity of the Lagrangian

$$\omega^2 = \frac{\text{Magnetic Energy}}{\text{Kinetic Energy}} = \frac{\int d^3\mathbf{r}\,[\nabla(\mathbf{b}\cdot\nabla\Phi)]^2}{4\pi\int d^3\mathbf{r}\rho(\nabla\Phi)^2/B^2}\,. \tag{1}$$

In Eq. (1), Φ is the wave electrostatic potential, and $\mathbf{b}$ is a unit vector along the unperturbed field $B\mathbf{b} = B_\phi\hat{\boldsymbol{\varphi}} + B_\theta\hat{\boldsymbol{\theta}}$. Because of the equilibrium toroidal symmetry, we expand $\Phi = \exp[i(n\varphi - \omega t)]\sum_m \phi_m(r)e^{-im\theta}$ and, by varying Eq. (1) with respect to ϕ_m, arrive at the mode equations valid to first order in ε:

$$\frac{d}{dr}\left(\frac{\omega^2}{v_A^2} - k_{\|m}^2\right)\frac{d\phi_m}{dr} - \frac{m^2}{r^2}\left(\frac{\omega^2}{v_A^2} - k_{\|m}^2\right)\phi_m + \varepsilon\frac{\omega^2}{v_A^2}\left[\frac{d^2\phi_{m+1}}{dr^2} + \frac{d^2\phi_{m-1}}{dr^2}\right] = 0\,. \tag{2}$$

In Eq. (2), $k_{\|m} = \frac{1}{R}\left(n - \frac{m}{q(r)}\right)$ with R and r the major and minor radii of the torus, and $q(r) = \frac{rB_\phi}{RB_\theta}$. The toroidal coupling factor is $\varepsilon = \sigma r/R \ll 1$, where the value of σ depends on the details of the equilibrium, e.g., $\sigma = 5/2$ near the TAE resonances for a low-beta, near-axis, Shafranov-shifted circular equilibrium.[7] In the cylindrical limit ($\varepsilon \to 0$), Eq. (2) has a singularity at the surface $\omega = k_{\|m}v_A$, which may be regularized by nonzero ε. Since the toroidal coupling is important only near the singularity, it is retained only in the highest order derivatives of $\phi_{m\pm1}$.

The essence of the TAE is seen by noting that for $\omega = \frac{v_A}{2Rq}$, modes m_0 and $m_0 + 1$

are both resonant at the point where $q = \frac{m_0+1/2}{n}$. Thus we look for a solution near $r = r_0$ where $q(r_0) = m_0/n \equiv q_0$ and use $\frac{1}{v_A^2} = \frac{1}{v_{A_0}^2}\left[1 + (q-q_0)\frac{d}{dq}\ln(1/v_A^2(q_0))\right]$. We write $R^2\omega^2 = \frac{v_A^2(r_0)}{4q_0^2}(1+\varepsilon g_0)$ where g_0 represents the shift of the eigenfrequency. In Eq. (2) we introduce $m = m_0 + \ell$, with $\ell \ll m_0$, and expand for each harmonic about the point r_ℓ where $k_{\|m_0+\ell} = 0$, i.e., $q(r_\ell) = \left(1 + \frac{\ell}{m_0}\right) q_0 \equiv q_\ell$. We find

$$R^2\left(\frac{\omega^2}{v_A^2(r)} - k_{\|m}^2(r)\right) = \frac{1}{q_\ell^2}\left[\frac{v_{A0}^2 q_\ell^2(1+\varepsilon g_0)}{4q_0^2 v_A^2(q_\ell)} - (x-\ell)^2\right] \approx \frac{1}{q_0^2}\left[\frac{1+\varepsilon g_\ell}{4} - (x-\ell)^2\right] , \quad (3)$$

where $x = n(q-q_0)$ and $g_\ell = g_0 + \frac{2\ell}{m_0\hat{\varepsilon}}$ with $\hat{\varepsilon} = \varepsilon\left[\frac{\partial \ln(q/v_A)}{\partial \ln q}\right|_0]^{-1}$. Equation (2) then becomes

$$\frac{d}{dx_\ell}\left(\frac{1+\varepsilon g_\ell}{4} - x_\ell^2\right)\frac{d\phi_\ell}{dx_\ell} - \frac{(\frac{1}{4} - x_\ell^2)}{s^2}\phi_\ell + \frac{\varepsilon}{4}\left[\frac{d^2\phi_{\ell+1}}{dx_\ell^2} + \frac{d^2\phi_{\ell-1}}{dx_\ell^2}\right] = 0 , \quad (4)$$

with $x_\ell = x - \ell$ and $s = d\ln q/d\ln r$. Toroidal coupling is only important at $x_\ell = \pm 1/2$ (coupling to the $\ell \pm 1$ harmonic). Near a singular layer (say $x_\ell = -1/2$), we find

$$\frac{d}{dy}\left[\left(\frac{\varepsilon g_\ell}{4} - y\right)\frac{d\phi_{\ell-1}}{dy} + \frac{\varepsilon}{4}\frac{d\phi_\ell}{dy}\right] = 0, \quad \frac{d}{dy}\left[\frac{\varepsilon}{4}\frac{d\phi_{\ell-1}}{dy} + \left(\frac{\varepsilon g_\ell}{4} + y\right)\frac{d\phi_\ell}{dy}\right] = 0 , \quad (5)$$

with $y = x - \ell + 1/2$. The first integrals are found for $\phi'_\ell \equiv d\phi_\ell/dy$:

$$\phi'_\ell = \left[yC_\ell - \frac{\varepsilon}{4}(C_{\ell-1} + g_\ell C_\ell)\right] \Big/ \left(y^2 + \frac{\varepsilon^2}{16}(1-g_\ell^2)\right) , \quad (6a)$$

$$\phi'_{\ell-1} = \left[yC_{\ell-1} + \frac{\varepsilon}{4}(C_\ell + g_\ell C_{\ell-1})\right] \Big/ \left(y^2 + \frac{\varepsilon^2}{16}(1-g_\ell^2)\right) . \quad (6b)$$

The integration constants C_ℓ and $C_{\ell-1}$ are the values of $y\phi'_\ell$ and $y\phi'_{\ell-1}$ away from the singular point. While $y\phi'$ is constant across the boundary, ϕ_ℓ and $\phi_{\ell-1}$ are discontinuous across the boundary layer of width $\varepsilon/4$, with jumps given by $\Delta\phi = \int_{-\infty}^{\infty}\phi'\,dy$ so that

$$\frac{\phi_\ell\Big|^+ - \phi_\ell\Big|^-}{\pi} = \frac{\Delta\phi_\ell}{\pi} = C_{\ell-1}\beta_\ell + C_\ell\alpha_\ell; \quad \frac{\Delta\phi_{\ell-1}}{\pi} = -C_{\ell-1}\alpha_\ell - C_\ell\beta_\ell , \quad (7)$$

with $\alpha_\ell = -g_\ell(1-g_\ell^2)^{-1/2}$ and $\beta_\ell = \alpha_\ell/g_\ell$. The branch of the square root is to be determined from the causality requirement that if $\omega_r > 0$ all functions of g are analytic in the upper half

plane. Hence along the real axis the square root is positive for $|g| < 1$ and is $-i\frac{g}{|g|}\sqrt{g^2-1}$ for $|g| > 1$, manifesting damping. Branch cuts are taken from $g_\ell = \pm 1$ to $-i\infty$.

Next we must ensure that all the harmonics ϕ_ℓ vanish as $x_\ell \to \pm\infty$. Except near the singularities at $x_\ell = \pm 1/2$ the harmonics obey Eq. (4) with $\epsilon = 0$. Thus, near the singularities, $\phi_\ell \sim (\ln|x_\ell^2 - \frac{1}{4}| + \Delta)C_\ell$ where Δ takes on various values depending on boundary conditions. Three characteristic values of Δ are: a) $\Delta_\infty(s)$, the value at $x_\ell^2 \gtrsim \frac{1}{4}$, for the solution that is well behaved as $|x_\ell| \to \infty$; (b) $\Delta_s(s)$, the value at $x_\ell \gtrsim -\frac{1}{2}$ for the solution that is symmetric about $x_\ell = 0$, i.e., $C_\ell(1/2) = C_\ell(-1/2)$, where we denote $C_\ell(-1/2) = C_\ell^-$ and $C_\ell(1/2) = C_\ell^+$; c) Similarly, $\Delta = \Delta_a(s)$ for the antisymmetric solution, with $C_\ell^+ = -C_\ell^-$.

We now trace the construction of ϕ_ℓ. For $x_\ell \lesssim -1/2$, we must have $\phi_\ell = C_\ell^-(\ln|x_\ell^2 - 1/4| + \Delta_\infty)$. For $x_\ell \gtrsim -1/2$, Eq. (7) gives $\phi_\ell = C_\ell^-(\ln|x_\ell^2 - 1/4| + \Delta_\infty + \pi\alpha_\ell + \pi\beta_\ell C_{\ell-1}^+/C_\ell^-)$. Since ϕ_ℓ can also be expressed as a superposition of symmetric and antisymmetric solutions, we have $\phi_\ell = \lambda_\ell C_\ell^-(\ln|x_\ell^2 - 1/4| + \Delta_s) + (1-\lambda_\ell)C_\ell^-(\ln|x_\ell^2 - 1/4| + \Delta_a)$ for $x_\ell \gtrsim -1/2$. Hence, $\Delta_\infty + \pi\alpha_\ell + \pi\beta_\ell C_{\ell-1}^+/C_\ell^- = \lambda_\ell\Delta_s + (1-\lambda_\ell)\Delta_a$. Further, for $x_\ell \lesssim 1/2$, we have $\phi_\ell = C_\ell^+\Big[\ln|1/4 - x_\ell^2| + (\lambda_\ell\Delta_s - (1-\lambda_\ell)\Delta_a)/(2\lambda_\ell - 1)\Big]$, with $C_\ell^+ = (2\lambda_\ell - 1)C_\ell^-$. Finally we must ensure after the jump at $x_\ell = 1/2$ that $\Delta = \Delta_\infty$; thus, $\frac{\lambda_\ell\Delta_s - (1-\lambda_\ell)\Delta_a}{2\lambda_\ell - 1} - \pi\alpha_{\ell+1} - \pi\beta_{\ell+1}\frac{C_{\ell+1}^-}{C_\ell^+} = \Delta_\infty$. Solving for λ_ℓ after eliminating the C^- coefficients, we obtain our basic recursion relationship between the C^+ coefficients (henceforth we drop the superscript) :

$$C_\ell\left[\frac{\beta_{\ell+1}^2 - (\alpha_{\ell+1} + \overline{\Delta})^2}{\overline{\Delta} + \alpha_{\ell+1}} + \frac{\tilde{\Delta}^2}{\overline{\Delta} + \alpha_\ell}\right] = C_{\ell-1}\left[\frac{\beta_\ell\tilde{\Delta}}{\overline{\Delta} + \alpha_\ell}\right] + C_{\ell+1}\left[\frac{\beta_{\ell+1}\tilde{\Delta}}{\overline{\Delta} + \alpha_{\ell+1}}\right] . \qquad (8)$$

We have defined $\overline{\Delta}(s) = \frac{1}{2\pi}[2\Delta_\infty - (\Delta_s + \Delta_a)]$ and $\tilde{\Delta}(s) = \frac{\Delta_s - \Delta_a}{2\pi}$, and their values are shown in Table I. Note that $\tilde{\Delta} < 0$, $\overline{\Delta} > 0$, and $\overline{\Delta} > |\tilde{\Delta}|$. The eigenvalue g_0 must be determined by the requirement that a solution to Eq. (8) can be found for which $C_\ell \to 0$ as $|\ell| \to \infty$. Note that if g_0 is an eigenvalue, then $g_0 + 2j/m_0\hat{\epsilon}$ with j any integer will also be an eigenvalue. Our principal interest is thus in the imaginary part of g_0.

For given s and $m_0\hat{\epsilon}$ Eq. (8) may be solved numerically. It can also be solved analytically

in two asymptotic limits. First consider the case $m_0\hat{\varepsilon} \ll 1$. Then all g_ℓ except g_0 will be large and for $\ell \neq 0$; $\alpha_\ell = -i, \beta_\ell = 0$. Then Eq. (8) is solved with only C_0 and C_{-1} nonzero, yielding

$$g_0^{(0)} = \lim_{m_0\hat{\varepsilon}\to 0} g_0 = -\frac{1-y^2}{1+y^2}\,, \tag{9}$$

with $y = \overline{\Delta} - \tilde{\Delta}^2/(\overline{\Delta} - i)$. Since $\overline{\Delta} > 0$, Eq. (9) gives $\mathrm{Im}\, g_0^{(0)} < 0$, implying damping. Values of the real and imaginary parts of $g_0^{(0)}$ are shown in Table I and provide an upper limit to the damping to be expected at finite $m_0\hat{\varepsilon}$.

We turn now to the interesting asymptotic case[8] $m_0\hat{\varepsilon} \gg 1$. In this limit the coefficients in Eq. (8) vary only slightly with ℓ and we employ a finite difference variant of WKB theory. We write Eq. (8) in the form $C_\ell(X_{\ell+1} + Y_\ell) = C_{\ell-1}\, W_\ell + C_{\ell+1}\, W_{\ell+1}$ where the subscripts on X, Y, and W indicate the dependence on ℓ arising from g_ℓ and hence α_ℓ and β_ℓ. Letting

$$C_\ell = \prod^{\ell} Q_j = \exp \sum^{\ell} \ln(Q_j) \approx \exp\left[\int^{\ell+\frac{1}{2}} d\ell'\, \ln\, Q(\ell')\right] \tag{10}$$

and then expanding in orders of $g' \equiv \frac{dg}{d\ell} = \frac{2}{m_0\hat{\varepsilon}}$ with $Q = Q_0 + Q_1 g'$, we have

$$Q_0(\ell) + \frac{1}{Q_0(\ell)} = \frac{X_\ell + Y_\ell}{W_\ell} \equiv 2f_\ell, \quad \frac{Q_1}{Q_0} = \frac{[X' - Q_0 W' - Q_0' W]}{W(Q_0 - 1/Q_0)}\,, \tag{11}$$

with the primes denoting differentiation with respect to g. Equation (11) is solved to find $Q_0 = f \pm \sqrt{f^2 - 1}$ with $f = [2g_\ell\overline{\Delta} + (1 - \overline{\Delta}^2 + \tilde{\Delta}^2)(1 - g_\ell^2)^{1/2}]/2|\tilde{\Delta}|$. For $|f| < 1$, we have $|Q_0| = 1$, representing an oscillating behavior of the C_ℓ, whereas for $|f| > 1$, as occurs for $|g| \sim 1$ (since $\overline{\Delta} > |\tilde{\Delta}|$), solutions are predicted that grow or decay as $|\ell| \to \infty$. We must choose the damped solution, corresponding to the minus sign in the expression for Q_0. Then, after some algebra and care with the singularity in W, Q_1 can be found from Eq. (11) and the integral $\int \frac{Q_1}{Q_0}\, dg$ performed to yield

$$C_{\ell-1} = \frac{\Gamma}{(f^2-1)^{1/4}} \frac{\left(g_\ell - \overline{\Delta}\sqrt{1-g_\ell^2}\right) \exp\left(\int^{g_\ell} \ln\left(f - \sqrt{f^2-1}\right) \frac{dg}{g'}\right)}{\left[1 + \tilde{\Delta}\sqrt{1-g_\ell^2}\,\left(f - \sqrt{f^2-1}\right)\right]^{1/2}}\,, \tag{12}$$

with Γ a normalizing constant. In the oscillating region

$$|C_{\ell-1}| \sim \frac{\Gamma}{(1-f^2)^{1/4}} \left| -g_\ell + \overline{\Delta}\sqrt{1-g_\ell^2} \right|^{1/2} , \tag{13}$$

and the usual WKB joining condition applies, viz., the solution $(f^2-1)^{-1/4}\exp[-\int(\cdots)]$ when $|f| \gtrsim 1$, behaves as $2(1-f^2)^{-1/4}\cos[\int(\cdots)]$ when $|f|<1$.

The global structure of the TAE mode can now be understood. Figure 1 shows a schematic plot of the toroidal shear Alfvén continuum resonance curves, $g_0^{\rm res}(x,\ell) = -(2\ell/m_0\hat{\varepsilon}) \pm [1+16(x-\ell-1/2)^2/\varepsilon^2]^{1/2}$ as a function of radial position $x = n(q-q_0)$, for a succession of poloidal harmonic numbers $m = m_0 + \ell$, where $q_0 = m_0/n$. (The expression for $g_0^{\rm res}$ follows from setting the denominator in Eq. (6) equal to zero.) For a given normalized frequency $g_0 = (\omega^2/\omega_0^2 - 1)/\varepsilon$, the harmonic $\phi_\ell(x)$ will have a dissipative response at the positions where continuum resonance, $g_0 = g_0^{\rm res}$, occurs. However, in the region where $g_\ell^2 < 1$, with $g_\ell = g_0 + 2\ell/m_0\hat{\varepsilon}$, no such resonance occurs, and these harmonics can combine to produce a global eigenmode. Each individual harmonic has only a limited radial extent, being localized where $|x-\ell| < 1/2$ and exponentiating to zero beyond this interval, as shown in Fig. 1. However, toroidal coupling permits the broad excitation of a global-type mode. In the region where $|f(\ell)| < 1$, the adjacent harmonic amplitudes have nearly equal amplitudes and shifted phase: i.e., for $C_\ell \propto \cos(\psi)$, then $C_{\ell\pm1} \propto \cos(\psi \pm \theta_\ell)$, with $\cos\theta_\ell = f(\ell)$ and ψ the phase. This "wave-like" pattern exists in the region $(m_0\hat{\varepsilon}/2)(g_- - g_0) < x < (m_0\hat{\varepsilon}/2)(g_+ - g_0)$, where $f(g_\pm) = \pm 1$. Outside of this region, the harmonic amplitudes C_ℓ are evanescent, with $C_{\ell\pm1}/C_\ell = \exp(-|\tilde{\theta}_\ell|)$, where the upper and lower signs correspond to $g > g_+$ and $g < g_-$, respectively, and $\cosh\tilde{\theta}_\ell = |f(\ell)|$. Since $|g_\pm| < 1$, the dissipation due to the continuum resonances at $g^2 = 1$ occurs where the mode amplitudes have exponentially decreased from their level in the wave-like region. Therefore, we expect the damping decrement to be proportional to a combination of the tunneling factors $\exp[-2\int_{g_\pm}^{1}(dg/g')\tilde{\theta}_\ell]$, evaluated from the wave-like region to the dissipation region.

In order to calculate the damping rate we construct a quadratic form by multiplying Eq. (8) by C_ℓ^* and summing over all ℓ to find:

$$I = \sum_\ell |C_\ell|^2 \left\{ \frac{1+\overline{\Delta}^2}{\overline{\Delta}+\alpha_{\ell+1}} - 2\overline{\Delta} \right\} + \sum_\ell |C_\ell|^2 \frac{\tilde{\Delta}^2}{\overline{\Delta}+\alpha_\ell} - \sum_\ell \left(C_\ell^* C_{\ell+1} + C_{\ell+1}^* C_\ell \right) \frac{\beta_{\ell+1}\tilde{\Delta}}{\overline{\Delta}+\alpha_{\ell+1}} = 0 \,. \tag{14}$$

For real g, I will have an imaginary part arising from α and β for $|g| > 1$. Moreover, for large $m_0\hat{\varepsilon}$ where C_ℓ decays rapidly as $|g|$ increases, the main contribution to Im I will come from $|g|$ close to 1. The damping rate will be determined from the relation (Im g) (dI/dg) + Im $I = 0$. Using Eqs. (12)–(14), we finally obtain an analytic expression for the damping rate $\gamma = \text{Im}\,\omega$ when $m_0\hat{\varepsilon} \gg 1$:

$$\text{Im}\, g^{\text{as}} = 2\gamma/\varepsilon\omega_0 = -\frac{G(s)}{(m_0|\hat{\varepsilon}|)^{3/2}} \left[\exp(-m_0|\hat{\varepsilon}|H_+) + \exp(-m_0|\hat{\varepsilon}|H_-) \right] \,, \tag{15}$$

with

$$G(s) = \frac{\sqrt{2}}{8\sqrt{\pi}} \frac{(1+\overline{\Delta}^2-\tilde{\Delta}^2)}{\sqrt{\overline{\Delta}^2-\tilde{\Delta}^2}} \left[\ln\left(\sqrt{\frac{\overline{\Delta}^2}{\tilde{\Delta}^2} - 1} + \frac{\overline{\Delta}}{|\tilde{\Delta}|} \right) \right]^{-3/2} \tag{16}$$

and

$$H_\pm(s) = \cosh^{-1} B - \frac{B\sqrt{B^2-1}}{A^2+B^2} + \frac{|A|}{A^2+B^2} \left[F(k,\phi) - E(k,\phi) \right] \mp \frac{A}{(A^2+B^2)^{1/2}} \left[K(k) - E(k) \right] \,. \tag{17}$$

Here $A = (1+\tilde{\Delta}^2-\overline{\Delta}^2)/2\tilde{\Delta}$, $B = -\overline{\Delta}/\tilde{\Delta}$, $k^2 = \frac{A^2+B^2-1}{A^2+B^2}$, $\phi = \sin^{-1}\frac{|A|}{\sqrt{A^2+B^2-1}}$, and $F(k,\phi)$ and $E(k,\phi)$ are the usual elliptic integrals, with $K(k) = F(k,\pi/2)$ and $E(k) = E(k,\pi/2)$. Values of $G(s)$ and $H_\pm(s)$ are shown in Table I.

Equation (15) gives our analytic result for the TAE damping at large $m_0\hat{\varepsilon}$. For small $m_0\hat{\varepsilon}$, Eq. (9) applies. An interpolation formula for the entire range is $(\text{Im}\, g)^{-1} = (\text{Im}\, g_0^{(0)})^{-1} + (\text{Im}\, g^{as})^{-1}$. Comparison of the interpolated analytic solution with the numerical solution of Eq. (8) shows the following features:

1) The analytic values asymptote satisfactorily to the numerical results at large $m_0\hat{\varepsilon}$. Since the large $m_0\hat{\varepsilon}$ analysis assumes a large exponentially decaying region it is quite sur-

prising that it seems to remain valid even for moderate and small $m_0\hat{\varepsilon}$, where typically the analytic damping rate may be 30% higher than the numerical values.

2) The numerical results show considerable oscillation in the damping rate as $m_0\hat{\varepsilon}$ is varied, which may be expected from the discrete nature of the sum for Im I from Eq. (14). At smaller s and $m_0\hat{\varepsilon}$ these oscillations are enhanced because in the numerics the sign of $\sqrt{g^2-1}$ is discontinuously changed when crossing the branch cuts, taken arbitrarily at $g_\ell = \pm 1 - i\gamma$ with γ real and positive. To refine this and to study whether interesting contributions to wave evolution arise from the branch cuts, it is necessary to resolve them by introducing finite Larmor radius or resistive effects, a subject to be considered in a subsequent paper.

Although our results are not valid if the overall eigenmode extends beyond the region where the linear expansion for $q^2(r)/v_A^2(r)$ is satisfied, the WKB procedure is easily generalized to treat this case, as will be discussed elsewhere.

Finally, we may draw three general conclusions. Damping is very weak at small shear ($s < 0.5$), which makes instability likely in the center of the discharge. Damping decreases strongly with m_0 (and hence n); however, the alpha drive dependence with m can be diminished due to FLR and banana effects,[9] while other non-ideal damping, e.g., due to the parallel electric field, will increase with m. It thus seems plausible that intermediate values such as those seen in recent experimental observations of the TAE instability[1,2] are most dangerous. Finally, we note that profiles with large $\hat{\varepsilon} = \varepsilon \left[\frac{\partial \ln(q/v_A)}{\partial \ln q}\right]^{-1}$ should be susceptible to alpha particle driven instability and alpha particle loss since the mode extends for large radial distances and the damping is small.

Acknowledgments

We are grateful to Drs. L. Chen, M. Chiu, Z. Guo, and F. Zonca for useful discussions and to J. Candy for the values in Table I. This work was supported by the U.S. Department of Energy under contract DE-FG05-80ET-53088 with the University of Texas at Austin and

contract DE-FG03-88ER-53275 with the University of California, San Diego.

References

1. K.L. Wong *et al.*, Phys. Rev. Lett. **66**, 1874 (1991).

2. W.W. Heidbrink, E.J. Strait, E. Doyle, and R. Snider, submitted to Nucl. Fusion.

3. M.N. Rosenbluth and P.H. Rutherford, Phys. Rev. Lett. **34**, 1428 (1975).

4. G.Y. Fu and J.W. Van Dam, Phys. Fluids B **1** 1919 (1989).

5. C.Z. Cheng, L. Chen, and M.S. Chance, Ann. Phys. (NY) **161**, 21 (1984).

6. J.A. Tataronis, J. Plasma Phys. **13**, 87 (1975).

7. H.L. Berk, J.W. Van Dam, Z. Guo, and D.M. Lindberg, submitted to Phys. Fluids B.

8. F. Zonca and L. Chen, Bull. Am. Phys. Soc. **35**, 2069 (1990).

9. H.L. Berk, B.N. Breizman, and H. Ye, submitted to Phys. Rev. Lett.

Table Caption

Values of the $\overline{\Delta}$ and $\tilde{\Delta}$ parameters, the normalized complex frequency $g_0^{(0)}$ of Eq. (9), and the G and $H_\pm$ functions in Eqs. (15)–(17), as functions of the shear s.

Figure Caption

Schematic plots of the toroidal shear Alfvén continuum resonance curves $g_0^{\rm res}(x,\ell)$ and of several TAE harmonics $\phi_\ell(x)$ and their global envelope, as functions of radial position $x = n(q-q_0)$.

Table I

s	$\overline{\Delta}$	$\tilde{\Delta}$	Re $g_0^{(0)}$	Im $g_0^{(0)}$	G	H_+	H_-
small s	$\pi s/4$	$-\exp(-1/s)$	$-1+\pi^2 s^2/8$	$-(16/\pi s)\exp(-2/s)$	$(s/2)^{1/2}\,\pi^{-3/2}$	$2/s$	$\pi^2\,s/8$
0.3	.2605	-.0621	-.8740	-.00329	.1366	4.515	.09512
0.4	.3831	-.1669	-.7553	-.02797	.1810	2.467	.07606
0.5	.5392	-.3206	-.6065	-.10238	.2337	1.270	.05844
0.6	.7326	-.5190	-.4620	-.2320	.2967	.6250	.04472
0.7	.9650	-.7594	-.3438	-.3968	.3712	.3072	.03455
0.8	1.2369	-1.0405	-.2532	-.5761	.4585	.1560	.02705
0.9	1.5483	-1.3613	-.1835	-.7586	.5594	.08320	.02150
1.0	1.8993	-1.7213	-.1282	-.9404	.6747	.04667	.01733
1.2	2.7193	-2.5578	-.0445	-1.298	.9520	.01686	.01169
1.4	3.6959	-3.5486	.0175	-1.648	1.2970	7.09×10^{-3}	8.24×10^{-3}
1.6	4.8281	-4.6929	.0662	-1.993	1.7161	3.35×10^{-3}	6.02×10^{-3}
1.8	6.1153	-5.9905	.1059	-2.334	2.2154	1.73×10^{-3}	4.53×10^{-3}
2.0	7.5570	-7.4413	.1389	-2.671	2.8010	9.58×10^{-4}	3.49×10^{-3}
2.2	9.1529	-9.0449	.1669	-3.007	3.4787	5.63×10^{-4}	2.75×10^{-3}
2.4	10.9027	-10.8016	.1910	-3.340	4.2544	3.47×10^{-4}	2.20×10^{-3}
2.6	12.8062	-12.7111	.2118	-3.671	5.1336	2.22×10^{-4}	1.79×10^{-3}
2.8	14.8632	-14.7735	.2301	-4.001	6.1220	1.47×10^{-4}	1.48×10^{-3}
3.0	17.0736	-16.9887	.2462	-4.330	7.2250	1.00×10^{-4}	1.23×10^{-3}
large s	$6s^2/\pi$	$-\overline{\Delta}+\dfrac{1}{\pi s}$	1	$-s\pi/2$	$\dfrac{\sqrt{2}}{4\pi^{3/2}}\,3^{5/4}\,s^{11/4}$	$\pi^2/(15\cdot 3^{5/2}\,s^{11/2})$	$\dfrac{1}{2\pi^2\,s^3}$

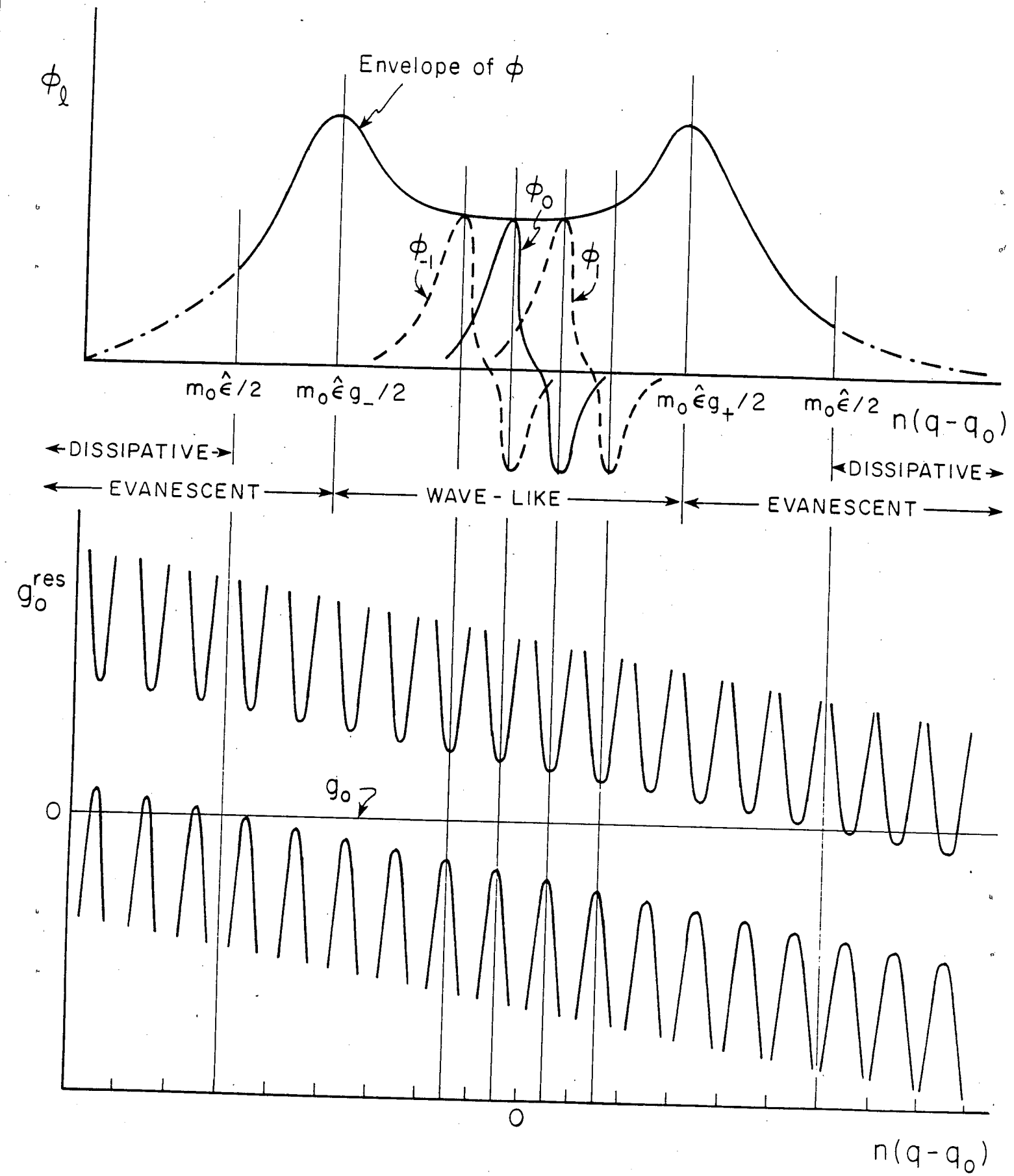
ϕ_l
Envelope of ϕ
ϕ_0
ϕ_{-1}
ϕ_1
$m_0\hat{\epsilon}/2$
$m_0\hat{\epsilon}g_-/2$
$m_0\hat{\epsilon}g_+/2$
$m_0\hat{\epsilon}/2$
$n(q-q_0)$
DISSIPATIVE
EVANESCENT
WAVE-LIKE
EVANESCENT
DISSIPATIVE
g_0^{res}
g_0
0
0
$n(q-q_0)$